

## Strain-controlled interface engineering of binding and charge doping at metal-graphene contacts

Wenbin Gong, Wei Zhang, Cuilan Ren, Xuezhi Ke, Song Wang, Ping Huai, Wenqing Zhang, and Zhiyuan Zhu

Citation: [Applied Physics Letters](#) **103**, 143107 (2013); doi: 10.1063/1.4823800

View online: <http://dx.doi.org/10.1063/1.4823800>

View Table of Contents: <http://scitation.aip.org/content/aip/journal/apl/103/14?ver=pdfcov>

Published by the [AIP Publishing](#)

---

### Articles you may be interested in

[Theoretical assessment of graphene-metal contacts](#)

J. Chem. Phys. **138**, 244701 (2013); 10.1063/1.4807855

[Fermi velocity modulation in graphene by strain engineering](#)

AIP Conf. Proc. **1512**, 360 (2013); 10.1063/1.4791060

[Atomic and electronic structure of graphene/Sn-Ni\(111\) and graphene/Sn-Cu\(111\) surface alloy interfaces](#)

Appl. Phys. Lett. **101**, 051602 (2012); 10.1063/1.4739475

[First-principles study of metal-graphene interfaces](#)

J. Appl. Phys. **108**, 123711 (2010); 10.1063/1.3524232

[First-principles investigation on bonding formation and electronic structure of metal-graphene contacts](#)

Appl. Phys. Lett. **94**, 103511 (2009); 10.1063/1.3095438

---

An advertisement for Physics Today. On the left, the 'physicstoday' logo is shown in white on a dark blue background. Below it, the text 'Comment on any Physics Today article.' is written in a large, white, serif font. On the right, there is a collage of overlapping images of article pages from Physics Today. A prominent red arrow points from the text towards the article pages. The visible text on the article pages includes the title 'Measured energy in Japan', the author 'David von Seggern', and a 'Comment on this article' section.

## Strain-controlled interface engineering of binding and charge doping at metal-graphene contacts

Wenbin Gong,<sup>1,2</sup> Wei Zhang,<sup>1,5,a)</sup> Cuilan Ren,<sup>1,5</sup> Xuezhi Ke,<sup>3,b)</sup> Song Wang,<sup>1,2</sup> Ping Huai,<sup>1,6</sup> Wenqing Zhang,<sup>4</sup> and Zhiyuan Zhu<sup>1,5</sup>

<sup>1</sup>Shanghai Institute of Applied Physics, Chinese Academy of Sciences, Shanghai 201800, China

<sup>2</sup>University of Chinese Academy of Sciences, Chinese Academy of Sciences, Beijing 100049, China

<sup>3</sup>Department of Physics, East China Normal University, Shanghai 200062, China

<sup>4</sup>Shanghai Institute of Ceramics, Chinese Academy of Sciences, Shanghai 200050, China

<sup>5</sup>Key Laboratory of Interfacial Physics and Technology, Chinese Academy of Sciences, Shanghai 201800, China

<sup>6</sup>Key Laboratory of Nuclear Radiation and Nuclear Energy Technology, Chinese Academy of Sciences, Shanghai 201800, China

(Received 3 July 2013; accepted 16 September 2013; published online 1 October 2013)

Strain effects on tuning the interface binding as well as the charge doping at metal-graphene contacts have been investigated by using density functional theory calculations. A realizable tensile strain is found to be very effective in enhancing the interface binding as well as shifting the Fermi level. Particularly, an enhancement of the binding energy up to 315% can be achieved because of the dipole-dipole interaction. Our results presented here show that strain is an efficient way to overcome the weak binding problem at metal-graphene interface, and will motivate active experimental efforts in improving the performance of graphene-based devices. © 2013 AIP Publishing LLC.  
[\[http://dx.doi.org/10.1063/1.4823800\]](http://dx.doi.org/10.1063/1.4823800)

Graphene-based devices have opened a crack in the door of post-silicon era.<sup>1–3</sup> An interface between graphene and other materials can bring additional control to the intrinsic properties of this unique 2-dimensional material,<sup>4,5</sup> and this is crucial in the creation of high-performance graphene devices. Therefore, interface engineering at contacts is a key step toward manipulating the electrical and optoelectronic applications of graphene devices. Particularly, the metallic contacts to a graphene layer can efficiently tune the electronic properties of graphene and be used as fundamental components in the devices. Pioneering works in the laboratories based on the metal-graphene contacts, such as high-performance transistors,<sup>6</sup> high-speed optical modulators,<sup>7</sup> ultrafast photodetectors,<sup>8</sup> and even integrated circuits,<sup>9</sup> have already revealed the prospective applications of graphene in the near future.

However, a huge challenge in the potential applications is the weak binding problem at the contacts. Up to date, a broad range of metals have not been considered appropriate as realistic materials at room temperature just due to their weak binding energy, although their contacts with graphene do not destroy the unique Dirac cone.<sup>10</sup> Along with fundamental understandings of the interaction between graphene and metals, several pathways have been explored to take care of this problem. Wang and Che emphasized the effects of metal-*d* states at metal-graphene contacts.<sup>11</sup> Gong *et al.* proposed a metal-graphene-metal sandwich structure and enhanced the binding energy between Cu-graphene interfaces by 65%.<sup>12</sup> In this letter, we demonstrate that an enhancement of interface binding up to 315% can be achieved by the application of strain. Moreover, strain shows its ability of tuning the interface electronic structures as well.

The employment of mechanical strain has already been found to be an economic and practical way to modify the properties of metal surfaces and graphene-related systems.<sup>13,14</sup> Mavrikakis *et al.* found that the chemical reactivity of metallic surfaces increased with the lattice expansion.<sup>15</sup> Zhou *et al.* confirmed strain not only stabilized the metal adatoms on graphene but also changed the properties of hydrogen storage and catalysis.<sup>16,17</sup> Li *et al.* found strain can enhance the NH<sub>3</sub> storage ability of Al atom on graphene.<sup>14</sup> Huang *et al.* reported a strain-controlled tuning of magnetism in metal-atom-decorated-graphene.<sup>18</sup> Merino *et al.*<sup>19</sup> and He *et al.*<sup>20</sup> suggested that strain drove the appearance of Moiré superstructures of graphene on transition metal surfaces. However, the quantitative analysis of strain effects on a metal-graphene interface, especially the changes in electronic properties, is still lacking. Herein, we focus our efforts on the realizable-strain-controlled interface engineering of a weakly-adsorbed metal-graphene interface.

For this purpose, we choose Cu (and some other metals: Al, Ag, and Au) as a model material in this density functional theory (DFT) study. The contact of graphene with Cu (111) constructs a prototypical interface with a weak interaction without sacrificing the intrinsic  $\pi$ -electron dispersion.<sup>4</sup> All calculations have been performed using the density functional theory as implemented in the VASP code.<sup>21,22</sup> The local-density approximations (LDA) has been proved to be more suitable for graphene-metal systems because it gives results with better accuracies than the generalized gradient approximations (GGA).<sup>4,10,23</sup> The recently-developed *van der Waals* (vdW) correction to GGA<sup>24,25</sup> even gives results that conflict with experimental observations for chemisorbed metal-graphene interfaces,<sup>26</sup> thus making the LDA more appropriate for this work. The Cu-graphene interface is modeled by a  $1 \times 1$  graphene unitcell adsorbed on a six-layer Cu (111) slab with other side a vacuum region of 15 Å.

<sup>a)</sup>Electronic mail: zhangwei@sinap.ac.cn

<sup>b)</sup>Electronic mail: xzke@phy.ecnu.edu.cn

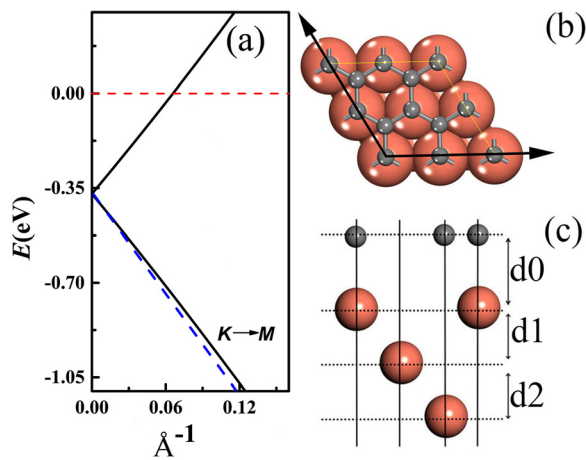


FIG. 1. (a) The band structure of Cu-graphene interface around Fermi energy close to  $K$  point. The slope of the blue dashed line is used to indicate the Fermi velocity of freestanding graphene. Fermi energy is at zero energy. The atomic structure of Cu-graphene interface from (b) top view and (c) side view. “ $d_0$ ,” “ $d_1$ ” and “ $d_2$ ” denote the distance between graphene and Cu, the first and second interlayer spacing in Cu, respectively.

Increasing the cell size up to  $3 \times 3$  only changes the binding energy per C atom by less than 0.01 eV, which assures that the  $1 \times 1$  cell is a reasonable choice. For such a small supercell, the Brillouin zone is sampled with a  $36 \times 36$   $k$ -point grid that explicitly includes the high-symmetry points. The binding energy per carbon atom in this study is calculated with respect to a free-standing graphene and bare Cu (111) substrate. The strain is introduced into the Cu-graphene interface by enlarging the simulation cell size, which is described by the in-plane lattice constant. The bottom two layers of the Cu substrate are fixed during geometry optimization; all the other atoms in the system are allowed to move. And total energy is converged to within  $10^{-5}$  eV/atom.

Figure 1 shows the band structure of Cu-graphene interface around the Fermi energy, as well as the employed geometry configuration of Cu (111)-graphene interface in this work. This structure of Cu-graphene interface is identified as the most stable configuration.<sup>10,23,27,28</sup> Due to the weak

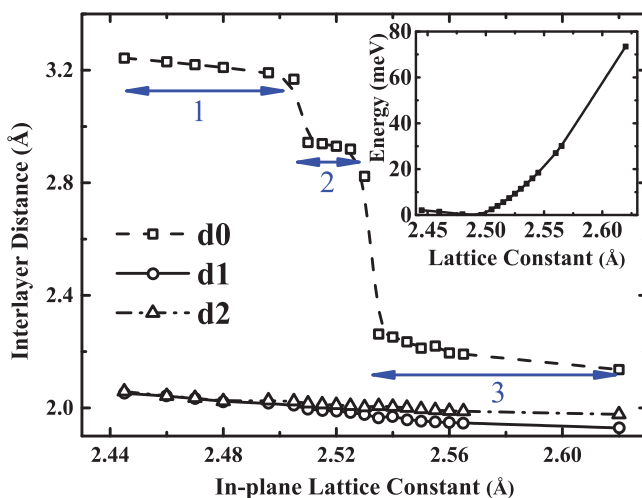


FIG. 2. Adsorption distances between Cu and graphene layers ( $d_0$ ), and the first two interlayer distances in Cu ( $d_1$  and  $d_2$ ), plotted as a function of in-plane lattice constant. Inset: Total energy differences per atom as a function of in-plane lattice constant.

interaction with Cu, graphene’s linearity of the band structure around the Fermi energy is preserved. However, the shift of the Dirac point indicates that electrons transfer from Cu to graphene when they contact with each other. The electron transfer is found to increase graphene’s carrier concentration, but slightly decrease the Fermi velocity, which is consistent with previous work.<sup>29</sup> Strain-induced changes of in-plane lattice constant is set from 2.45 Å to 2.62 Å here. The interface system was then relaxed under the strain, we got the optimized distance “ $d_0$ ,” as well as the distances of the first two interlayer spacing of Cu “ $d_1$ ” and “ $d_2$ ,” as shown in Fig. 2. It is found that “ $d_1$ ” and “ $d_2$ ” decrease continuously around 2 Å without surprise when strain is strengthened.<sup>30,31</sup> However, the distance “ $d_0$ ” between Cu and graphene exhibits two interesting sudden drops and three platforms (1, 2, 3) under strain. These two sudden drops occur at 2.51 Å and 2.54 Å, respectively. The difference of “ $d_0$ ” between the platform 1 and the platform 2 is about 0.20 Å, and that between the platform 2 and the platform 3 is approximately 0.80 Å. The maximum total energy difference per atom under the strain in our study is less than 0.08 eV (as shown in the inset in Fig. 2), indicating that the range of strain applied here is realizable.

The changes of distance between graphene and Cu indicate the changes of binding energy and the shift of Fermi level.<sup>10,32</sup> We have calculated the binding energy and the Fermi level shift as a function of the in-plane lattice constant as illustrated in Fig. 3. The magnitude of the binding energy of the Cu-graphene interface increases with the strain as shown by the dashed-dotted line in the figure. When the strain makes the in-plane lattice constant change from 2.45 Å to 2.62 Å, the magnitude of binding energy increases from 0.03 eV to 0.14 eV (with an enhancement of 315%). Considering the weak binding problem, the strain appears to provide a simple way to enhance the interface binding and thus increases the range of available metals for applications in graphene-based devices. The energy curve is composed of three parts with two knee points at 2.51 Å and 2.54 Å. Each part corresponds to the three platforms in Fig. 2, although the first two parts are hard to be distinguished by eye. The binding energy is almost constant at first with the increasing strain, however, its magnitude increases greatly as the in-

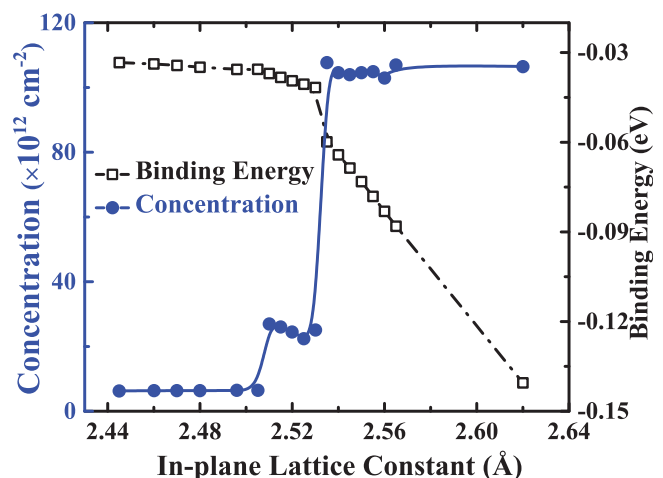


FIG. 3. Plot of the binding energy (dashed line), and carrier concentration (solid line) as a function of the in-plane lattice constant.

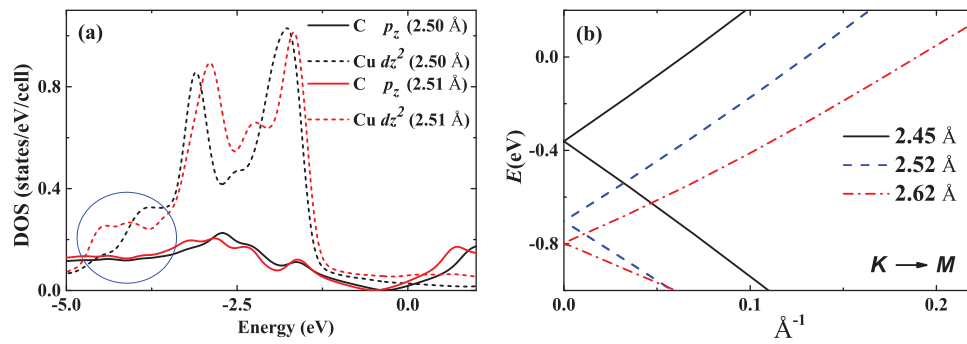


FIG. 4. Electronic structures of Cu-graphene interface: (a) PDOS on  $p_z$  state of graphene and  $dz^2$  state of Cu (1st layer) with in-plane lattice constants of 2.50 Å and 2.51 Å. (b) Band structures of Cu-graphene interface around Fermi energy near  $K$  point. Solid, dashed, and dashed-dotted lines correspond to the in-plane lattice constants of 2.45 Å (in platform 1), 2.52 Å (in platform 2) and 2.62 Å (in platform 3), respectively.

plane lattice constant becomes larger than 2.54 Å. This result suggests that the mechanism of interaction in each individual platform should be different from each other.

In order to understand the first sudden drop between the platforms 1 and 2 in Fig. 2, the electronic structures of the interface are calculated. The projected density of states (PDOS) is plotted in Fig. 4(a), in which the carbon  $p_z$  ( $\pi$ ) state and Cu  $dz^2$  state under the strain (2.50 Å and 2.51 Å) are shown. The  $dz^2$  state shows pronounced changes, in particular, a broadened DOS in the energy range from  $-5.0$  eV to  $-3.0$  eV. We think this broadened DOS is responsible for increasing the binding energy, and thus causing the sudden drop. It is noticed that the envelope of the PDOS for carbon is similar to that of the freestanding graphene. To further check the unique electronic properties, the band structures of the interface under the strain are plotted in Fig. 4(b). It is found that both the Dirac point and the linear dispersion of graphene around the Fermi energy are still kept. However, the change of the slope of the linear line indicates that the Fermi velocity is decreased. The Fermi velocity decreases maximally by  $\sim 35\%$ , compared with the freestanding graphene. According to the electronic transport theory in graphene,<sup>33</sup> the minimum Fermi velocity in our study still results in an electrical conductivity as high as approximately  $0.4 \times 10^6 \Omega^{-1} \text{cm}^{-1}$ , which is only slightly smaller than that of the pure Cu crystal ( $0.6 \times 10^6 \Omega^{-1} \text{cm}^{-1}$ ).

To explain the mechanism for the second sudden drop between the platforms 2 and 3 in Fig. 2, a plane-averaged electron densities analysis was performed. Khomyakov *et al.* defined the plane-averaged electron densities in Ref. 10 to study the charge transfer upon formations of a variety of metal-graphene interfaces. Here, we introduced the plane-averaged electron densities to visualize the strain-induced electron redistribution. Figure 5 shows the plane-averaged electron density differences ( $\Delta n$ ) with different in-plane lattice constants: 2.45 Å in (a) and 2.54 Å in (b). When the lattice constant is set as 2.45 Å,  $\Delta n$  is localized near the interface, and it has the shape of a simple dipolar charge distribution with the maxima about  $2 \times 10^{-3} \text{e}/\text{Å}$ . However, when the in-plane lattice constant increases to 2.54 Å, the charge distribution is strongly perturbed. A much more complex profile of the charge distribution is showed. The maximum of  $\Delta n$  becomes about  $5 \times 10^{-3} \text{e}/\text{Å}$ . Comparing Fig. 5(b) with Fig. 5(a), it is easy to find that electrons are depleted from the Cu (111) surface and accumulated on the

graphene sheet under strain. This results in a negative charge accumulation on the graphene, and positive one on the Cu layer. Therefore, the dipole-dipole interaction is established to significantly enhance the binding, which results in the graphene sheet moving closer to Cu substrate. Walter *et al.* have already reported that in the absence of strain, the majority of electron transferred from the Cu to graphene comes from the bulk instead of surface electrons.<sup>34</sup> However, our finding shows that the electron transfer from the Cu surface state does occur when the strain is applied. And the surface state plays a decisive role in establishing the dipole-dipole interaction.

In addition to enhancing the binding, the strain also can be used to tune the carrier concentration of graphene. The carrier concentration as a function of strain is shown in solid line in Fig. 3. It is found that the carrier concentration is closely related to the adsorption distances of graphene on Cu substrate. The smaller the adsorption distance is, the more the carriers transfer from Cu to graphene. With the change of the adsorption distances, the carrier concentration also shows three platforms and two sudden changes. The numerical analysis indicates that the strain-induced changes of carrier concentration can differ by two orders of magnitude. As the in-plane lattice constant is smaller than 2.51 Å (platform 1), the carrier concentration is of the order of  $10^{12} \text{cm}^{-2}$ . With the

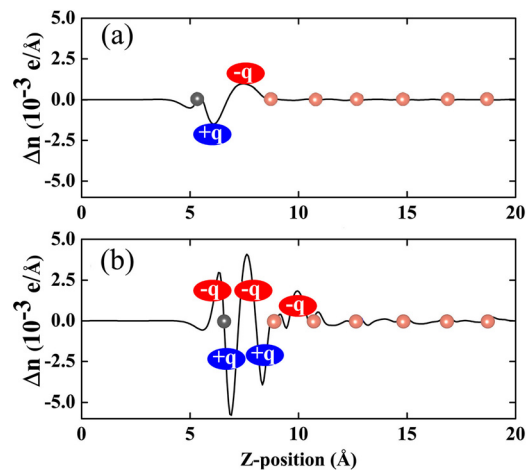


FIG. 5. Plane-averaged electron density differences as a function of  $Z$ -position (perpendicular to the interface) with two different in-plane lattice constants: (a) 2.45 Å and (b) 2.54 Å. The black and cinnamon balls denote the  $Z$ -positions of graphene and Cu layers, respectively.

TABLE I. The strain-induced binding energy change ( $\Delta BE$ ) and the distance change ( $\Delta d$ ) between graphene and metal substrates. The in-plane lattice constants are set to be 4.90 Å and 5.24 Å for the case without and with strain, respectively. The negative  $\Delta BE$  and  $\Delta d$  denote the increased binding strengths and the decreased distances. The corresponding percent differences are shown in the brackets.

	Ag	Au	Al
$\Delta BE$ (meV)	-22 (71%)	-16 (53%)	-4 (15%)
$\Delta d$ (Å)	-0.47 (14%)	-0.29 (9%)	0.05 (2%)

continued increase of strain, the carrier concentration reaches  $10^{13} \text{ cm}^{-2}$  (platform 2), and even  $10^{14} \text{ cm}^{-2}$  (platform 3). These results suggest that the strain is an efficient way to tune the carrier concentration of graphene at the metal-graphene interfaces.

Finally, we also explore the strain effects on some other metal-graphene contacts (Al, Ag, and Au), and the results confirm the universality of the strain-enhanced interface binding. Since graphene adsorbed on Al, Ag, and Au is modeled in a  $2 \times 2$  supercell, the range of the in-plane lattice constant is doubled here (4.90 Å  $\sim$  5.24 Å). The strain-induced binding energy change ( $\Delta BE$ ) and the distance change ( $\Delta d$ ) at the interfaces are listed in Table I. The  $\Delta BE$  of the three metal-graphene interfaces are all negative values, indicating the binding enhancement under strain. And we noticed that  $\Delta BE$  of noble metal-graphene interface (Ag, Au) is almost an order larger than that of Al-graphene interface. Similar phenomenon is also presented in  $\Delta d$ . The distances between graphene and noble metals (Ag, Au) both show apparent decreases (0.29 Å at least) under strain, whereas  $\Delta d$  of the Al-graphene interface is only about 0.05 Å. We deduced that this difference should be ascribed to the different electron configurations of metal atoms on one hand. These noble metal atoms all process  $d^{10}s^1$  electron configuration, while the Al atom has a quite different one  $s^2p^1$ . On the other hand, the noble metal (111) surfaces are all the  $s$ - $p$  derived Shockley states, and they play a decisive role as discussed above. Extra calculations, including vdW corrections, were also performed in our study, although they provided no better accuracy than the LDA. The calculations did not change our basic results of the strain-induced interface binding enhancement as well as the Fermi level shift.

In conclusion, by using DFT calculations, we have studied the strain effects on the metal-graphene interface engineering of binding and charge doping. The applied strain is found to effectively tune both the interface binding and the shift of Fermi level. Especially, an enhancement of binding energy up to 315% for Cu-graphene interface can be achieved because of the dipole-dipole interaction. In contrast to the unstrained condition, the (111) surface states of noble metals are found to play a decisive role in establishing the dipole-dipole interaction. Our results presented here show that strain is an optional way to overcome the weak binding problem at metal-graphene interface, and will motivate active experimental efforts in improving the performance of graphene-based devices.

This work is supported by the National Basic Research Program of China (Grant No. 2010CB934504), strategically Leading Program of the Chinese Academy of Sciences (Grant No. XDA02040100), the National Natural Science Foundation of China (11075196, 11005142), the Shanghai Municipal Science and Technology Commission (11ZR1445200), and CAS Hundred Talents Program. The Shanghai Supercomputing Center is acknowledged for allocation of computing time.

<sup>1</sup>P. Avouris, *Nano Lett.* **10**, 4285 (2010).

<sup>2</sup>R. S. Singh, V. Nalla, W. Chen, W. Ji, and A. T. S. Wee, *Appl. Phys. Lett.* **100**, 093116 (2012).

<sup>3</sup>Z. Y. Fang, Z. Liu, Y. M. Wang, P. M. Ajayan, P. Nordlander, and N. J. Halas, *Nano Lett.* **12**, 3808 (2012).

<sup>4</sup>G. Giovannetti, P. A. Khomyakov, G. Brocks, V. M. Karpan, J. van den Brink, and P. J. Kelly, *Phys. Rev. Lett.* **101**, 026803 (2008).

<sup>5</sup>E. Voloshina and Y. Dedkov, *Phys. Chem. Chem. Phys.* **14**, 13502 (2012).

<sup>6</sup>Y. M. Lin, C. Dimitrakopoulos, K. A. Jenkins, D. B. Farmer, H.-Y. Chiu, A. Grill, and P. Avouris, *Science* **327**, 662 (2010).

<sup>7</sup>M. Liu, X. Yin, E. Ulin-Avila, B. Geng, T. Zentgraf, L. Ju, F. Wang, and X. Zhang, *Nature* **474**, 64 (2011).

<sup>8</sup>F. Xia, T. Mueller, Y.-M. Lin, A. Valdes-Garcia, and P. Avouris, *Nat. Nanotechnol.* **4**, 839 (2009).

<sup>9</sup>E. Guerriero, L. Polloni, M. Bianchi, A. Behnam, E. Carrion, L. G. Rizzi, E. Pop, and R. Sordan, *ACS Nano* **7**, 5588–5594 (2013).

<sup>10</sup>P. A. Khomyakov, G. Giovannetti, P. C. Rusu, G. Brocks, J. van den Brink, and P. J. Kelly, *Phys. Rev. B* **79**, 195425 (2009).

<sup>11</sup>Q. J. Wang and J. G. Che, *Phys. Rev. Lett.* **103**, 066802 (2009).

<sup>12</sup>C. Gong, D. Hinojos, W. Wang, N. Nijem, B. Shan, R. M. Wallace, K. Cho, and Y. J. Chabal, *ACS Nano* **6**, 5381 (2012).

<sup>13</sup>K. S. Kim, Y. Zhao, H. Jang, S. Y. Lee, J. M. Kim, K. S. Kim, J. H. Ahn, P. Kim, J. Y. Choi, and B. H. Hong, *Nature* **457**, 706 (2009).

<sup>14</sup>Y. Li, A. D. Sarkar, B. Pathak, and R. Ahuja, *Appl. Phys. Lett.* **102**, 243905 (2013).

<sup>15</sup>M. Mavrikakis, B. Hammer, and J. K. Nørskov, *Phys. Rev. Lett.* **81**, 2819 (1998).

<sup>16</sup>M. Zhou, Y. Lu, C. Zhang, and Y. Feng, *Appl. Phys. Lett.* **97**, 103109 (2010).

<sup>17</sup>M. Zhou, A. Zhang, Z. Dai, Y. Feng, and C. Zhang, *J. Phys. Chem. C* **114**, 16541 (2010).

<sup>18</sup>B. Huang, J. J. Yu, and S. H. Wei, *Phys. Rev. B* **84**, 075415 (2011).

<sup>19</sup>P. Merino, M. Svec, A. L. Pinardi, G. Otero, and J. A. Martin-Gago, *ACS Nano* **5**, 5627 (2011).

<sup>20</sup>R. He, L. Zhao, N. Petrone, K. S. Kim, M. Roth, J. Hone, P. Kim, A. Pasupathy, and A. Pinczuk, *Nano Lett.* **12**, 2408 (2012).

<sup>21</sup>G. Kresse and J. Furthmüller, *Phys. Rev. B* **54**, 11169 (1996).

<sup>22</sup>P. E. Blöchl, *Phys. Rev. B* **50**, 17953 (1994).

<sup>23</sup>L. Adamska, Y. Lin, A. J. Ross, M. Batzill, and I. I. Oleynik, *Phys. Rev. B* **85**, 195443 (2012).

<sup>24</sup>S. Grimme, *J. Comput. Chem.* **27**, 1787 (2006).

<sup>25</sup>A. Tkatchenko and M. Scheffler, *Phys. Rev. Lett.* **102**, 073005 (2009).

<sup>26</sup>M. Vanin, J. J. Mortensen, A. K. Kelkkanen, J. M. Garcia-Lastra, K. S. Thygesen, and K. W. Jacobsen, *Phys. Rev. B* **81**, 081408 (2010).

<sup>27</sup>J. Lahiri, T. Miller, L. Adamska, I. Oleynik, and M. Batzill, *Nano Lett.* **11**, 518 (2011).

<sup>28</sup>M. Fuentes-Cabrera, M. I. Baskes, A. V. Melechko, and M. L. Simpson, *Phys. Rev. B* **77**, 035405 (2008).

<sup>29</sup>D. C. Elias, R. V. Gorbachev, A. S. Mayorov, S. V. Morozov, A. A. Zhukov, P. Blake, L. A. Ponomarenko, I. V. Grigorieva, K. S. Novoselov, F. Guinea, and A. K. Geim, *Nat. Phys.* **7**, 701 (2011).

<sup>30</sup>W. Köster and H. Franz, *Mettall. Rev.* **6**, 1 (1961).

<sup>31</sup>E. Friis, R. Lakes, and J. Park, *J. Mater. Sci.* **23**, 4406 (1988).

<sup>32</sup>J. Slawinska, P. Dabrowski, and I. Zasada, *Phys. Rev. B* **83**, 245429 (2011).

<sup>33</sup>S. Sarma, S. Adam, E. Hwang, and E. Rossi, *Rev. Mod. Phys.* **83**, 407 (2011).

<sup>34</sup>A. L. Walter, S. Nie, A. Bostwick, K. S. Kim, L. Moreschini, Y. J. Chang, D. Innocenti, K. Horn, K. F. McCarty, and E. Rotenberg, *Phys. Rev. B* **84**, 195443 (2011).